International Journal of Nanomedicine

Dovepress
open access to scientific and medical research

Open Access Full Text Article

ORIGINAL RESEARCH

Water-Soluble Carbon Dots in Cigarette Mainstream Smoke: Their Properties and the Behavioural, Neuroendocrinological, and Neurotransmitter Changes They Induce in Mice

This article was published in the following Dove Press journal:
International Journal of Nanomedicine

Yan Zhao[1]
Fang Lu[2]
Yue Zhang[2]
Meiling Zhang[1]
Yusheng Zhao[3]
Juan Luo[1]
Hui Kong[1]
Huihua Qu[4]

[1]School of Traditional Chinese Medicine, Beijing University of Chinese Medicine, Beijing, 100029, People's Republic of China; [2]School of Life Science, Beijing University of Chinese Medicine, Beijing, 100029, People's Republic of China; [3]School of Chinese Materia Medica, Beijing University of Chinese Medicine, Beijing, 100029, People's Republic of China; [4]Beijing Institute of Traditional Chinese Medicine, Beijing University of Chinese Medicine, Beijing, 100029, People's Republic of China

Background: It is well known that smoking is harmful to health; however, it can also ameliorate anxiety. To date, it is unclear whether any nanoparticles found in cigarette mainstream smoke (CS) contribute to this effect.

Aim: The aim of this study was to assess the particle composition of CS to identify novel anti-anxiety components.

Methods: Carbon dots (CDs) from CS (CS-CDs) were characterised using high-resolution transmission electron microscopy, Fourier-transform infrared, ultraviolet, fluorescence, X-ray photoelectron spectroscopy, X-ray diffraction and high-performance liquid chromatography. The anti-anxiety effects of CS-CDs in mouse models were evaluated and confirmed with the elevated plus maze and open-field tests.

Results: The quantum yield of CS-CDs was 13.74%, with a composition of C, O, and N. In addition, the surface groups contained O-H, C-H, C=O, C-N, N-H, C-O-C, and COO− bonds. Acute toxicity testing revealed that CS-CDs had low in vitro and in vivo toxicity within a certain concentration range. The results of the elevated plus maze and open-field tests showed that CS-CDs had a significant anti-anxiety effect and a certain sedative effect in mice. The mechanism of these effects may be related to the decrease in glutamate levels and promotion of norepinephrine production in the mouse brain, and the decrease in dopamine in mouse serum due to CS-CDs.

Conclusion: CS-CDs may have anti-anxiety and certain sedative effects. This study provides a new perspective for a more comprehensive understanding of the components, properties, and functions of CS. Furthermore, it offers a novel target for the development of smoking cessation treatments, such as nicotine replacement therapy.

Keywords: carbon dots, cigarette mainstream smoke, anxiety, smoking cessation therapy

Background

Based on World Health Organization (WHO) data, tobacco is one of the greatest global health threats ever faced by the public; approximately one person dies every 6 s because of tobacco, including direct tobacco use and exposure to second-hand smoke, accounting for one in 10 adult deaths, which amounts to approximately 6 million deaths per year. [1,2]

Over 3800 chemical constituents have been identified in tobacco; moreover, cigarette mainstream smoke (CS) contains at least 4800 chemical constituents

Correspondence: Hui Kong; Huihua Qu
Beijing University of Chinese Medicine, No. 11, Bei San Huan Dong Lu, Chaoyang District, Beijing, 100029, People's Republic of China
Tel +86 10-62486705
Email doris7629@126.com; quhuihuadr@163.com

submit your manuscript | www.dovepress.com
DovePress
http://doi.org/10.2147/IJN.S291670

because of chemical reactions occurring at temperatures up to 950°C.[3] In particular, CS is an aerosol of liquid droplets suspended within a mixture of gases and semi-volatile compounds.[4] Previous studies have reported that 44 substances in CS are associated with smoking-related diseases.[3]

Despite the known disadvantages of smoking, a considerable number of people indulge in smoking or are unsuccessful at quitting the habit. This because smoking provides mood relief and pleasure to individuals.[5,6] In addition, nicotine, which is present in tobacco as well as CS, stimulates the release and transmission of dopamine in the brain. This release, is responsible for creating pleasure and forming a nicotine reward mechanism, a key mechanism for the nicotine addiction role of dopamine in the behavioural actions of nicotine related to addition.[7] However, it is still unclear what components of CS relieve emotional distress (anxiolytic-like effect).

In recent years, a new type of carbon nanomaterial, called carbon dots (CDs), has been developed. The particle size of CDs is typically approximately 10 nm. Because of their special optical and excellent biological properties, CDs have important applications in biomedical sensors, biosensors, therapeutic drug encapsulation, and disease diagnosis.[8,9] Moreover, some studies have reported that CDs may also have medicinal properties. For example, CDs prepared from ginger can inhibit the growth of human hepatocellular carcinoma cells in nude mice,[10] and CDs derived from egg yolk oil,[11] schizonepetae herba carbonisata,[12] pollen typhae carbonisata,[13] phellodendri cortex,[14] cirsii japonica herba carbonisata,[15] and schizonepetae spica carbonisata have hemostatic effects.[16] Furthermore, CDs from CS have broad-spectrum antimicrobial activities.[17] CDs derived from aurantii fructus immaturus carbonisata have antihyperuricemic and anti-gouty arthritis activities.[18] Charred fructus crataegi CDs have maltase and sucrase inhibitory activities and hypoglycaemic effects.[19] Moreover, CDs derived from Puerariae lobatae radix have anti-gout effects[20] and those from phellodendri chinensis cortex carbonisata can prevent deinagkistrodon acutus venom-induced acute kidney injury.[21] In particular, aggregated single-walled carbon nanotubes may have therapeutic effects for the treatment of methamphetamine addiction by oxidation of methamphetamine-enhanced extracellular dopamine in the striatum.[22] In summary, CDs from different sources have certain pharmacodynamic effects; therefore, these CDs could be new sources of drug discovery. While it has been observed that smoking has anxiolytic-like effects, thus far, whether the CDs in CS play a role in realising these properties of CS has not been explored.

Thus, in this study, we aimed to identify CS-CDs with low toxicity and anti-anxiety effects. In addition, nicotine replacement therapy is used as an effective way to quit smoking; however, nicotine is addictive. Hence, we sought to discover a substance that could replace nicotine as a novel therapeutic target for smoking cessation studies.

Materials and Methods

Chemicals

Cigarettes were purchased from a local store (tar content, 5mg·stick^{-1}. Zhongnanhai, Shanghai Tobacco Group Co., Ltd. Shanghai, China). Nicotine was purchased from Beijing Honghu United Chemical Products Co. Ltd. (Beijing, China). Diazepam tablets were purchased from Beijing Yimin Pharmaceutical Co. Ltd. (Beijing, China). Dialysis membranes (1 k Da) were purchased from Beijing Ruida Henghui Technology Development Co., Ltd. (Beijing, China). RPMI-1640 medium, Dulbecco's Modified Eagle's Medium (DMEM), foetal bovine serum (FBS), antibiotics, and antimycotics were obtained from Gibco BRL (Gaithersburg, MD, USA). Enzyme-linked immunosorbent assay (ELISA) kits were used to measure the concentration of 5-hydroxytryptamine (5-HT), norepinephrine (NE), corticotropin releasing hormone (CRH), corticosterone (CORT), adrenocorticotropic hormone (ACTH) and dopamine (DA); these were purchased from Cloud-Clone Corp. (Katy, TX, USA). CCK-8 was purchased from Dojindo Molecular Technologies, Inc. (Kumamoto, Japan).

Analytical-grade chemical reagents were obtained from Sinopharm Chemical Reagents Beijing (Beijing, China). All experiments were performed using deionised water.

Cells and Mice

RAW 264.7 cells were purchased from the Shanghai Institute of Cell Biology Chinese Academy of Sciences (Shanghai, China).

This study was performed in accordance with the Guide for the Care and Use of Laboratory Animals and approved by the Committee of Ethics of Animal Experimentation of the Beijing University of Traditional Chinese Medicine (approval number: BUCM-4-2018091109-3038). Male ICR mice, weighing 25.1 ±

1.0 g, were purchased from the Laboratory Animal Center, Weitong Lihua, with a Laboratory Animal Certificate of Conformity. They were maintained under the following conditions: temperature, 24.0 ± 1.0 °C; relative humidity, 55–65%; 12-h light/dark cycle; and ad libitum access to food and water.

Instrumentation

The morphology, size, and microstructure of CS-CDs were obtained using high-resolution transmission electron microscopy (HRTEM, JEN-1230; Japan Electron Optics Laboratory, Tokyo, Japan). Fluorescence images were acquired using an OLYMPUS IX73 fluorescent microscope (Tokyo, Japan). Pure water was produced using a circulating water-type multi-purpose vacuum pump (Great Wall Scientific Industry, Henan, China). UV-Vis spectroscopy was performed using a CECIL instruments spectrophotometer (Cambridge, UK). FTIR spectroscopy was performed using a Thermo spectrometer (Thermo Fisher Scientific, Waltham, MA, USA). Raman spectra were obtained using a Lab RAM HR800 Raman spectrometer (Jobin-Yvon, HORIBA Group, Longjumeau, France) with an incident laser light having a wavelength of 514 nm. X-ray diffraction (XRD) spectra were obtained using an Ultima IV X-ray diffractometer (Rigaku, Tokyo, Japan).

An Agilent series 1260 high-performance liquid chromatography (HPLC) instrument (Agilent, Waldbronn, Germany) equipped with a column compartment, autosampler, degasser, quaternary pump, and diode-array detector was used to measure amounts of nicotine and other small molecule compounds. Quantification of amino acids in mice brains was performed using ultra-performance liquid chromatography-tandem mass spectrometer (UPLC-MS/MS, Waters ACQUITY UPLC I-CLASS) with a tandem mass spectrometer (Xevo TQ-S Micro).

A spectrophotometric microtiter reader (Multiskan MK3; Thermo Fisher Scientific) was used to measure optical density (OD). An electro-heating standing temperature cultivator (DRP-9082) was purchased from Samsung Laboratory Instrument Co., Ltd. (Shanghai, China). A high-speed refrigerated centrifuge (HC-2518R) was purchased from Anhui USTC Zonkia Scientific Instruments Co., Ltd. Anhui, China. A circulating water multipurpose vacuum pump was purchased from Zhengzhou Great Wall Scientific Industrial and Trade Co., Ltd.

Preparation of CS-CDs

A cigarette was lit, and the vacuum circulation pump was activated to simulate smoking. The smoke was dissolved into a water solution in the kettle; Images of the smoking cycle simulator created in the laboratory are shown in Figure 1. We burned two cigarettes at the same time to improve efficiency. We replaced deionised water in an absorption bottle (200 mL) with 20 sticks of burned cigarettes (each cigarette contained approximately 0.75 g tobacco). A total of 600 cigarettes were burned, and all water in the absorption bottles was collected to concentrate to 360 mL. Immediately after this, the solution was extracted three times using ethyl acetate, followed by dialysis using a 1 k Da molecular weight cut-off dialysis membrane. The dialysis water was changed every 8 h. After 7 days of dialysis, the solution inside the dialysis membrane was centrifuged at 8910 *g* for 10 min. Next, the supernatant was collected,

Figure 1 Preparation of CS-CDs.

concentrated to 71 μg·mL^{-1}, and stored at 4°C until further analysis.

Characterisation of CS-CDs

The morphology, size, and microstructure of CS-CDs were acquired via HRTEM.UV-vis spectroscopy and fluorescence spectroscopy were employed to investigate the optical properties of the CS-CDs, where in water was used as a blank control. The FTIR spectrometer was employed to identify the organic functional groups in the CDs within a spectral window of 400–4000 cm^{-1}. The surface composition and elemental analyses of the CDs were performed via X-ray photoelectron spectroscopy (XPS) (ESCALAB 250Xi, Thermo Fisher Scientific, Fremont, CA) with a mono X-ray source Al Kl excitation (1486.6 eV).[23–26]

HPLC was employed to identify the compounds existing in the smoke water before and after purification. For the HPLC analysis, a 15-μL water extract was filtered through 0.22-mm cellulose acetate membrane filters and injected into the Reliasil-C18 column (250 × 4.6 mm, 5 μm, Orochem, Naperville, IL) and eluted at 24°C. The mobile phase consisted of 0.25% H_3PO_4 water (solvent A) and acetonitrile (solvent B). The elution system was as follows: 0–6 min, 0–12% of B; 6–10 min, 12–18% of B; and 10–30 min, 18–58% of B. The flow rate was 1.0 mL·min^{-1}, and the detection wavelengths were 210, 254, 320, and 365 nm.[27]

The obtained CS-CDs and quinine sulphate were dissolved in double distilled water and in 0.1 M H_2SO_4, respectively. The quantum yield of CS-CDs was then determined as previously reported by Hu et al.[28] In particular, the integrated photoluminescence intensities and absorbency values of CS-CDs were measured, and then compared to the reference, quinine sulphate.

Cell Viability Assay

RAW 264.7 cells were cultured in DMEM supplemented with 10% FBS, 100 mg·mL^{-1} streptomycin, and 100 IU·mL^{-1} penicillin in a 5%-CO_2 atmosphere at 37°C.

Cell viability in RAW 264.7 cells was measured using the CCK-8 assay kit. In particular, the cells were seeded at a density of 1 × 10^5 cells·mL^{-1} in 96-well culture plates in serum-free media and incubated in a humidified incubator at 37°C for 24 h prior to treatment with phosphate-buffered saline (PBS) as the negative control, and CS-CDs and nicotine as the positive controls. After incubation, 10 μL of CCK-8 was added to each well, and they were allowed to stand for 4 h, after which the OD was measured at 490 nm.[12,29]

Acute Toxicity Experiment in Mice

ICR mice, weighing 25.1 ± 1.0 g, were randomly divided into three groups and injected (intraperitoneally; i.p.) with 5× purified CS-CDs (355 μg·mL^{-1}), 10× purified CS-CDs (710 μg·mL^{-1}), or 20× purified CS-CDs (1420 μg·mL^{-1}) (n = 5 per group). In this study, the maximum dose of the CS-CD efficacy test was used as the basis for the calculated dose of the toxicity test, namely the 1× dose. These mice were housed for 7 days in breeding boxes after injection. Weight, diet, behaviour, and death were recorded daily. Following this period, the mice were euthanised, and sections were obtained and visualised.[30]

Behavioural Tests in Mice

Anxiety in the mice was measured using the open-field test (OFT) and elevated plus maze test (EPMT). ICR mice, weighing 25.1 ± 1.0 g, were randomly assigned to treatment groups (n = 8 per group). In particular, mice were treated (i.p.) with saline, diazepam (100 μg·mL^{-1}), or CS-CDs (71, 35.5, or 17.8 μg·mL^{-1}). Saline and CS-CDs were administered 10 min before the behavioural tests, while diazepam was administered 30 min before the tests. As mood is affected soon after smoking, the time for starting the measurement after administration was shortened compared with diazepam. Each mouse performed only one test in this study.

The OFT apparatus was a non-transparent container (50 × 50 × 30 cm) with a black floor divided into 25 zones (10 × 10 cm).[31] The container was illuminated using a 60-W floor lamp, which provided illumination in the testing room only. A digital camera controlled by a computer was placed 2.6 m above the centre of the container. The 16 zones that were adjacent to the walls represented the safe area (peripheral area), and the nine zones in the centre represented the exposed area (central area). Each mouse was placed individually into the centre of the container and allowed to explore the container freely for 5 min. Mice were recorded using the digital camera on the ceiling and videos were analysed using EthoVision XT 7 software (Noldus Information Technology, Wageningen, Netherlands).

The EPMT apparatus consisted of two non-transparent opposite open arms (30 × 5 cm) and two opposite closed arms (30 × 5 × 25 cm) in a cross

configuration. The arms were connected via a central platform (5 × 5 cm), and they were elevated by 45 cm above the floor.[32] The maze was illuminated using a 60-W floor lamp. A digital video camera was suspended above the maze to record the movements of the mice. Each mouse was placed gently in the centre of the platform facing an open arm, and their actions were video recorded for 5 min. The time spent in the open arms, and the number and percentage of entries into open arms were calculated from the video recordings to study the anxiolytic-like activity in the mice. If a mouse fell from the maze, it was removed from the experiment.

Estimation of Serum CRH, ACTH, CORT, and DA

After the EPMT test, mouse blood was collected from the venous sinus retro-orbitally into serum tubes immediately, allowed to clot for 2 h at 25°C, and then centrifuged at 802 *g* for 10 min at 4°C. The serum was separated and stored at –80°C for further analysis. CRH, ACTH, CORT, and DA concentrations were determined using commercially available, enzyme-linked immunosorbent assay (ELISA) kits according to the manufacturer's instructions. The absorbance of each sample was measured at a wavelength of 450 nm. CRF, ACTH and DA are presented as $pg \cdot mL^{-1}$, and CORT is presented as $ng \cdot mL^{-1}$.[31]

The mice that were administered saline and had EPMT were used as model groups (Model), while those that were not subjected to EPMT were used as normal saline groups (NS). The mice that were given CS-CDs (71 $\mu g \cdot mL^{-1}$) were used as CS-CD groups (CS-CDs).

Determination of Neurotransmitter Concentrations in Mouse Brains

Preparation of Mouse Brain Tissue Samples

After the EPMT test, and mouse blood collection, their brains were isolated after decapitation. These brains were stored at −80°C until further analysis. The experimental group is the same as above.

Quantification of Glutamate (Glu) and γ-Aminobutyric Acid (GABA)

Samples for UPLC-MS/MS analysis were prepared by placing 50 mg of mouse brain in a tube with 1 mL of acetonitrile and water (1:1); this mixture was homogenised by shaking for 30 min and centrifuged at 13,200 rpm for 10 min. The supernatant was further diluted 6-fold with acetonitrile and water (1:1) before analysis.

Glu and GABA quantifications of mouse brains were performed using a UPLC-MS/MS with an electrospray ionisation (ESI +) ion source and analytical column (Acquity UPLC BEH Amide, 1.7 μm, 100 × 2.1 mm, water, Milford, MA, USA). The mobile phase included A (water and 0.1% formic acid) and B (acetonitrile with 2.5 $mmol \cdot L^{-1}$ ammonium formate and 0.1% formic acid) solutions. A volume of 1 μL of the extract was injected into the system. Spectrometric parameters were as follows: the capillary voltage was set to 1.5 kV with a cone voltage of 10 V and cone gas flow of 10 $L \cdot h^{-1}$. The ion source temperature was 150°C, and the desolvation temperature was 400°C; The desolvation gas flow was 800 $L \cdot h^{-1}$. The mass spectrometer was operated in multiple reaction monitoring (MRM) mode with an ion pair for Glu of 148.1 > 102.1, and GABA of 104.101 > 87.1.

Quantification of 5-Hydroxytryptamine (5-HT) and Norepinephrine (NE)

Samples for ELISA analysis were prepared by weighing 300 mg of mice brain placed into a 2-mL centrifuge tube, which was then homogenised with 3 mL of PBS. After centrifuging the tube for 10 min in a high-speed refrigerated centrifuge (10,000 rpm, 4°C), the 5-HT and NE in the supernatant was measured using commercially available, ELISA kits according to the manufacturer's instructions. The OD of each sample was measured at a wavelength of 450 nm.

Statistical Analysis

Statistical analysis was performed using the Statistical Package for the Social Sciences (SPSS, version 16.1, Chicago, IL, USA) software. Normally distributed variables and those with homogeneous variances are expressed in the mean ± standard deviation (SD) form. Multiple comparisons were performed using one-way analysis of variance (ANOVA) followed by the least significant difference test. Data were considered statistically significant if $p < 0.05$.

Results

Characterisation of CS-CDs

The obtained HRTEM results (Figure 2A–C) revealed that CS-CDs were nearly spherical with a size distribution range of 1–6 nm, the average of the CS-CDs diameter is about 3.23 nm and that these CS-CDs were dispersed uniformly at nanoscale. In addition, the CS-CDs had a lattice spacing of 0.282 nm (Figure 2C). Furthermore,

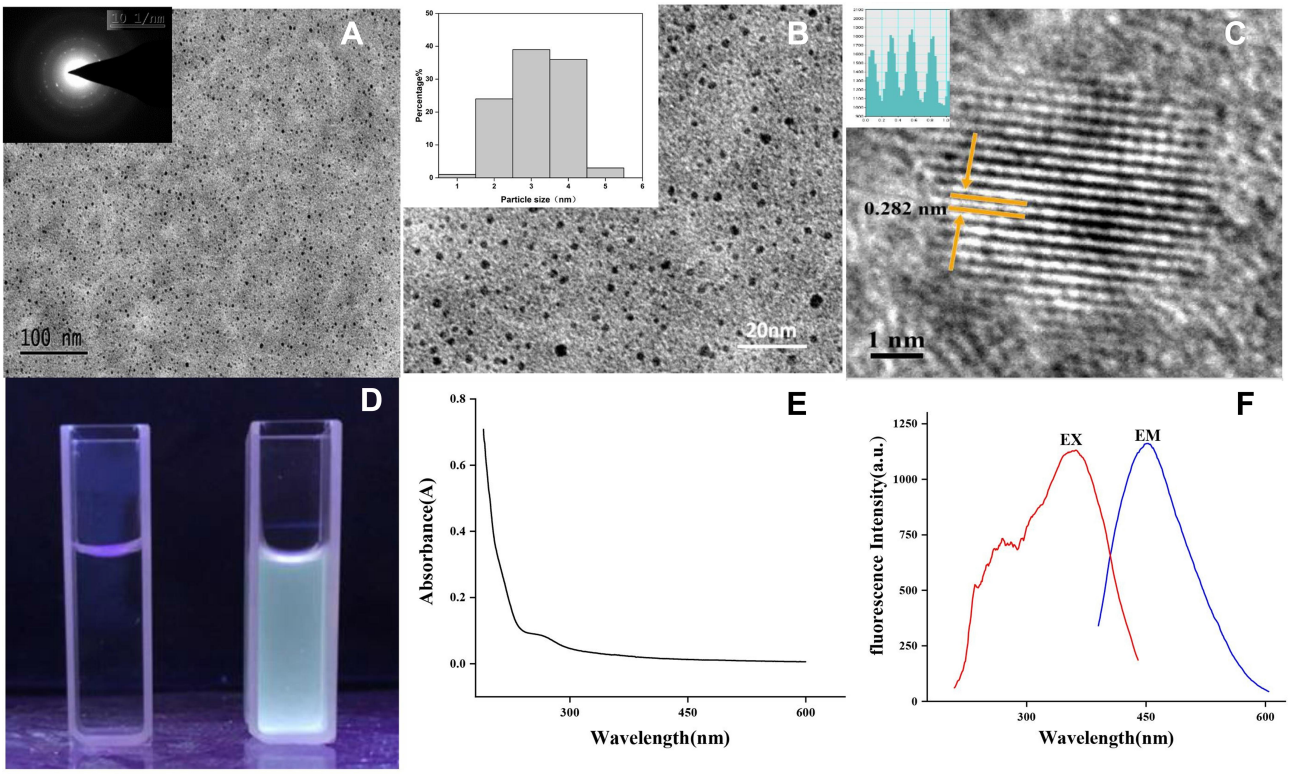

Figure 2 Characterisation of CS-CDs. (**A**) HRTEM images of CS-CDs displaying ultra-small particles. Inset: electron diffraction image of selected area. (**B**) HRTEM images of CS-CDs. Inset: histogram depicting particle size distribution. (**C**) HRTEM images of CS-CDs. Inset: line profiles of the corresponding HRTEM images of CS-CDs. (**D**) Images obtained using 365-nm light. (**E**) UV–vis and (**F**) fluorescence spectra.

Selected Area Electron Diffraction (SAED) patterns were also obtained using the same instrument as that used for HRTEM. The corresponding SAED patterns reveal the formation of an amorphous carbon phase and hexagonal carbon.[33,34] In a quartz glass bottle, CS-CDs had a light cyan fluorescence at 365 nm (Figure 2D).The quantum yield of CS-CDs was 13.74%.

The UV spectrum of CS-CDs is shown in Figure 2E. The UV–Vis spectrum showed a clear adsorption peak at 260 nm, which can be ascribed to the π–π* transition of the aromatic C=C bonds. Moreover, the emission spectrum of CS-CDs showed the strongest emission and excitation at approximately 452 and356 nm, respectively (Figure 2F).

The Raman spectrum is shown in Figure 3A; the peaks centred at 1365 cm^{-1} and 1583 cm^{-1} are the D and G bands of sp2 carbon materials, respectively. The intensity ratio ID/IG was 0.56, indicating a good crystalline nature for CS-CDs.[35,36]

The 2θ angle in the XRD spectrum (Figure 3B) of CS-CDs was 31.589°, while the atomic lattice spacing was 0.283 nm, which is in agreement with the result of 0.282 nm measured on the HRTEM magnified image.

The FTIR spectrum (Figure 3C) revealed the presence of O-H groups at 3422 cm^{-1}, and C-H groups at 2922 cm^{-1} and 1384 cm^{-1}. Furthermore, the peaks at 1632 cm^{-1} and 1402 cm^{-1} were identified as C=O, C-N, N-H, C-O-C, and COO^{-} groups, while the peaks at 1384 cm^{-1} and 1033 cm^{-1} were attributed to the benzene structure of CS-CDs.[11,14,37]

The CS-CD surface composition and elemental analysis were characterised using the XPS technique. Figure 4A shows that the CS-CDs were primarily composed of the elements C, O, and N with relative percentage compositions of 72.74%, 23.87%, and 2.61%, respectively. In particular, the elements C, O, and N might correspond to C–C, C=C, C=O, C–N, N–H, C–OH, and C–O–C bonds (Figure 4B–D).This result was in accordance with the surface composition of the CS-CDs shown in the FTIR analysis.

In addition, small amounts of P and S were also observed in the CS-CDs with relative percentage compositions determined to be 0.63% and 0.29%, respectively, which could be derived from tobacco combustion products. In particular, tobacco containsS[38] and P.[39] Thus, during tobacco combustion in the process of smoking, these two elements might become part of

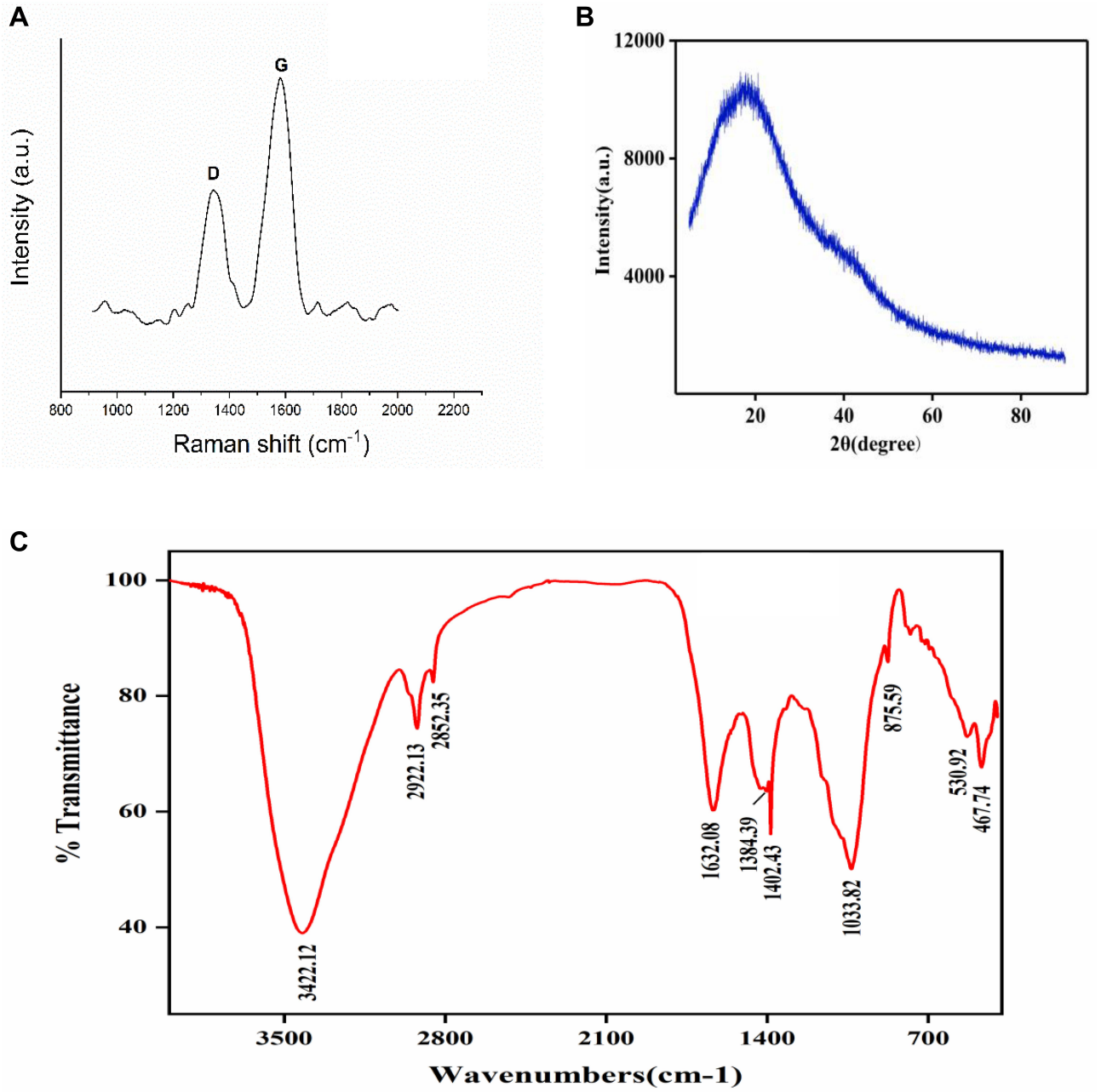

Figure 3 (**A**) Raman spectrum of CS-CDs. (**B**) XRD pattern spectrum of CS-CDs. (**C**) FTIR spectra of CS-CDs.

the CDs during their formation. In Figure 4E, the peaks at 133.1 and 133.9 eV could be attributed to P−C and P−O bonds, respectively.[40] Furthermore, in Figure 4F, the S2p peak could be divided into five components with peaks located at 163.1, 164.2, 167.5, 168.3, and 169.2 eV, that could be ascribed to -S2p2/3-, -S2p1/2-, -C−SO2-, -C-SO3-, and C−SO4- bonds, respectively.[41]

Moreover, the HPLC results showed several compounds in the collected smoke water before purification, such as nicotine (highest peak in Figure 5A); however, we detected no active small molecule compounds in the collected smoke water after purification (Figure 5B).

In summary, the purified CS-CDs solution have no nicotine or other small molecule compounds, and the CS-CDs have graphite structure cores consisting primarily of N and O with traces of S and P containing functional groups, such as hydroxyl groups, carbonyl groups, and amino groups on their surface.

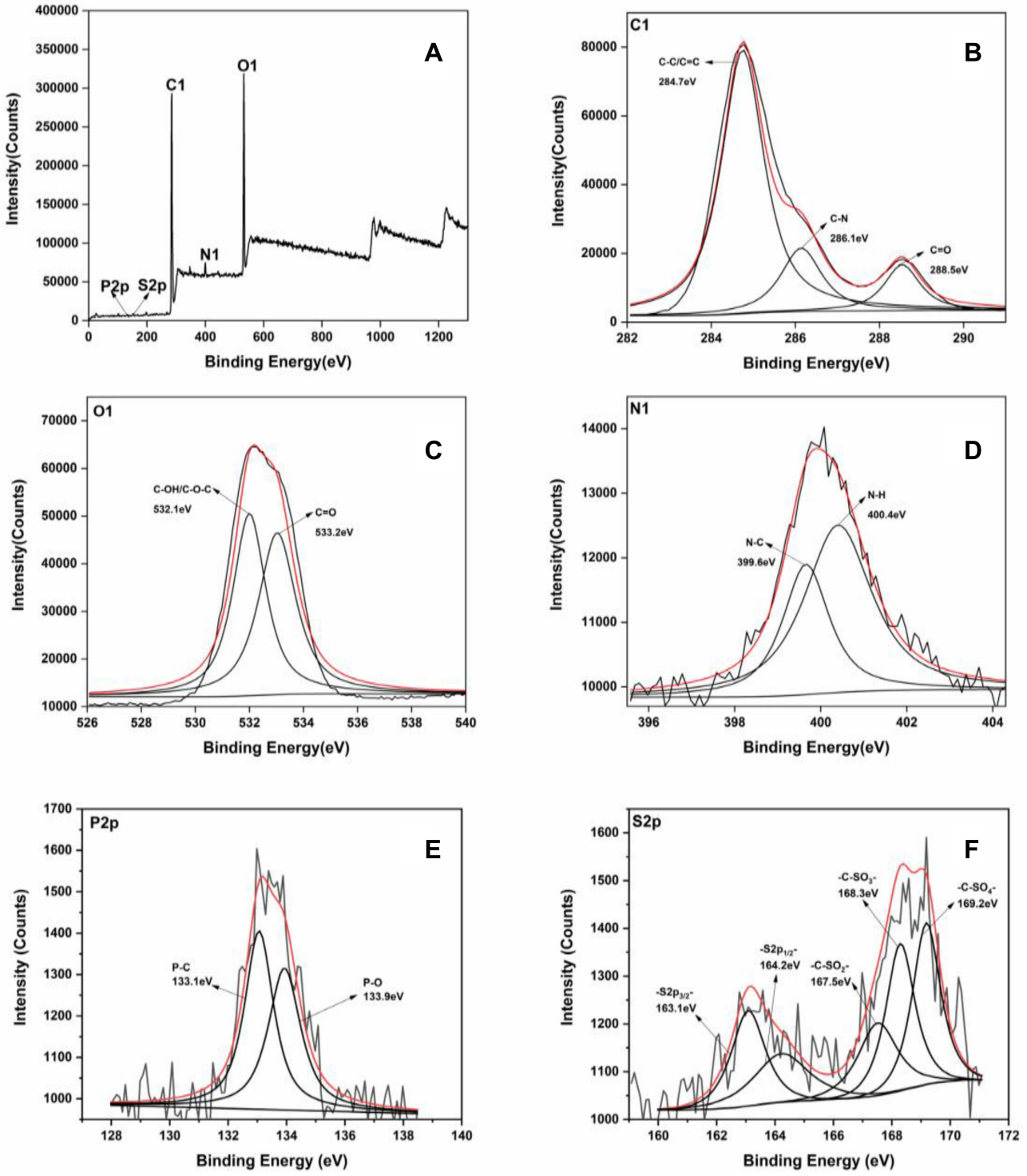

Figure 4 XPS of CS-CDs. (**A**) XPS survey spectra. (**B**) C 1s, (**C**) N1s, (**D**) O 1s,(**E**) P2p, (**F**) S2p XPS spectra.

Acute Toxicity in vitro

The ODs of PBS, CS-CDs, and nicotine were recorded. The viability of RAW 264.7 cells was calculated as follows:

$$\text{Viability\%} = (OD_{sample}\text{-}OD_{PBS})/OD_{PBS}\times 100$$

Figure 6 shows the viability of cells treated with CS-CDs at different concentrations (2.3–71 $\mu g \cdot mL^{-1}$) for 24 h. The CS-CDs promoted RAW 264.7 cell growth at concentrations below 35.5 $\mu g \cdot mL^{-1}$ and inhibited cell proliferation at 71 $\mu g \cdot mL^{-1}$. This trend is consistent with the effect of nicotine.

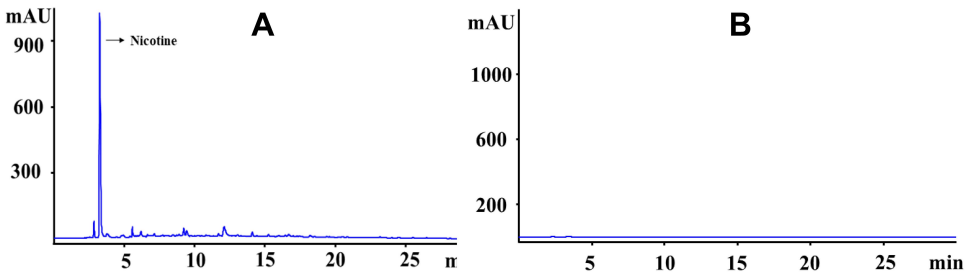

Figure 5 HPLC chromatograms of CS-CDs (**A**) before purification, and (**B**) after purification.

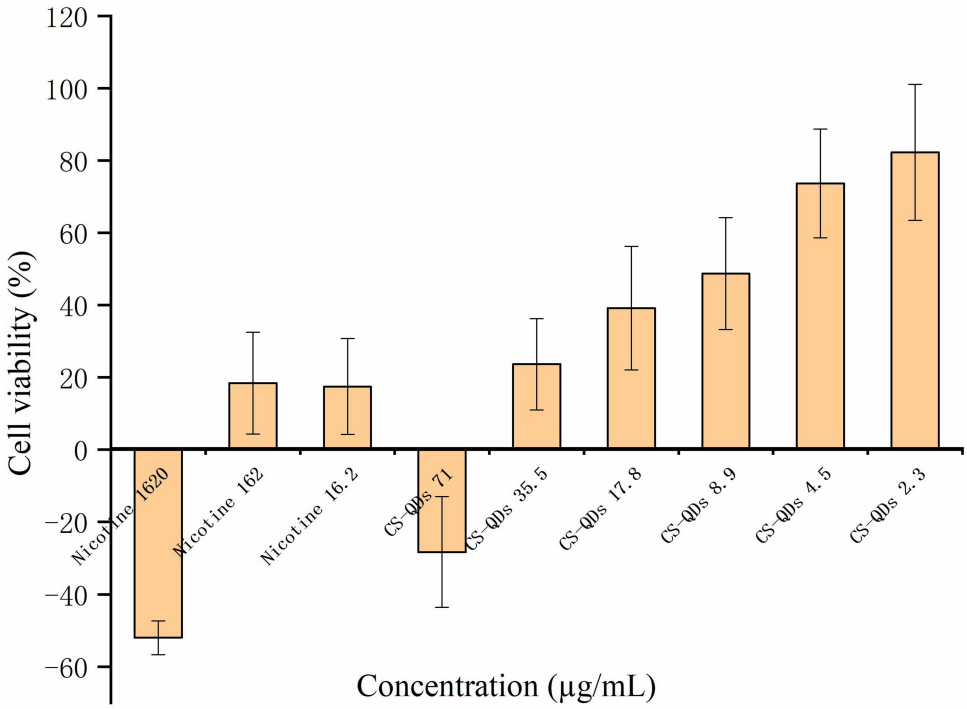

Figure 6 RAW 264.7 cell viability after incubation with various concentrations of cigarettes smoke carbon dots (CS-CDs), PBS (negative control) or nicotine (positive control) for 24 h The cell viability of RAW 264.7 cells was calculated by the OD of the sample minus the OD of the negative control, PBS, then divided by the OD of the negative control, and then multiplied by 100. The value of cell activity was greater than zero, indicating that it can promote cell proliferation, and less than zero, indicating that it can inhibit cell proliferation.

Acute Toxicity in vivo

No mice died during 7 days after 355 $\mu g \cdot mL^{-1}$, 710 $\mu g \cdot mL^{-1}$, and 1420 $\mu g \cdot mL^{-1}$ administration of CS-CDs (i.p.). In addition, there were no differences in weight, diet, or behaviour. Dissection did not reveal any congestion in the lungs, heart, liver, spleen, or kidney, indicating that CS-CDs toxicity was low.

Anti-Anxiety Effects of CS-CDs

The EPMT results are shown in Figure 7A. Mice injected with 71 $\mu g \cdot mL^{-1}$ CS-CDs or 100 $\mu g \cdot mL^{-1}$ diazepam spent significantly more time in the open arms ($p < 0.01$) than those in the NS group. Furthermore, mice that were administered 35.5 $\mu g \cdot mL^{-1}$ and 17.8 $\mu g \cdot mL^{-1}$ CS-CDs spent more time in the open arms than those in the NS group; however, this difference did not reach statistical significance. Thus, the effect of CS-CDs on time spent in the open arms was dose-dependent.

Figure 7B and C show that the number and percentage of entries into the open arms by mice injected with CS-CDs or diazepam decreased compared to those in the NS group. A significant difference was found between the NS and high-dose CS-CD groups. This finding indicates that the locomotor activity of mice decreased and that CS-CD injection produced a certain sedative effect.

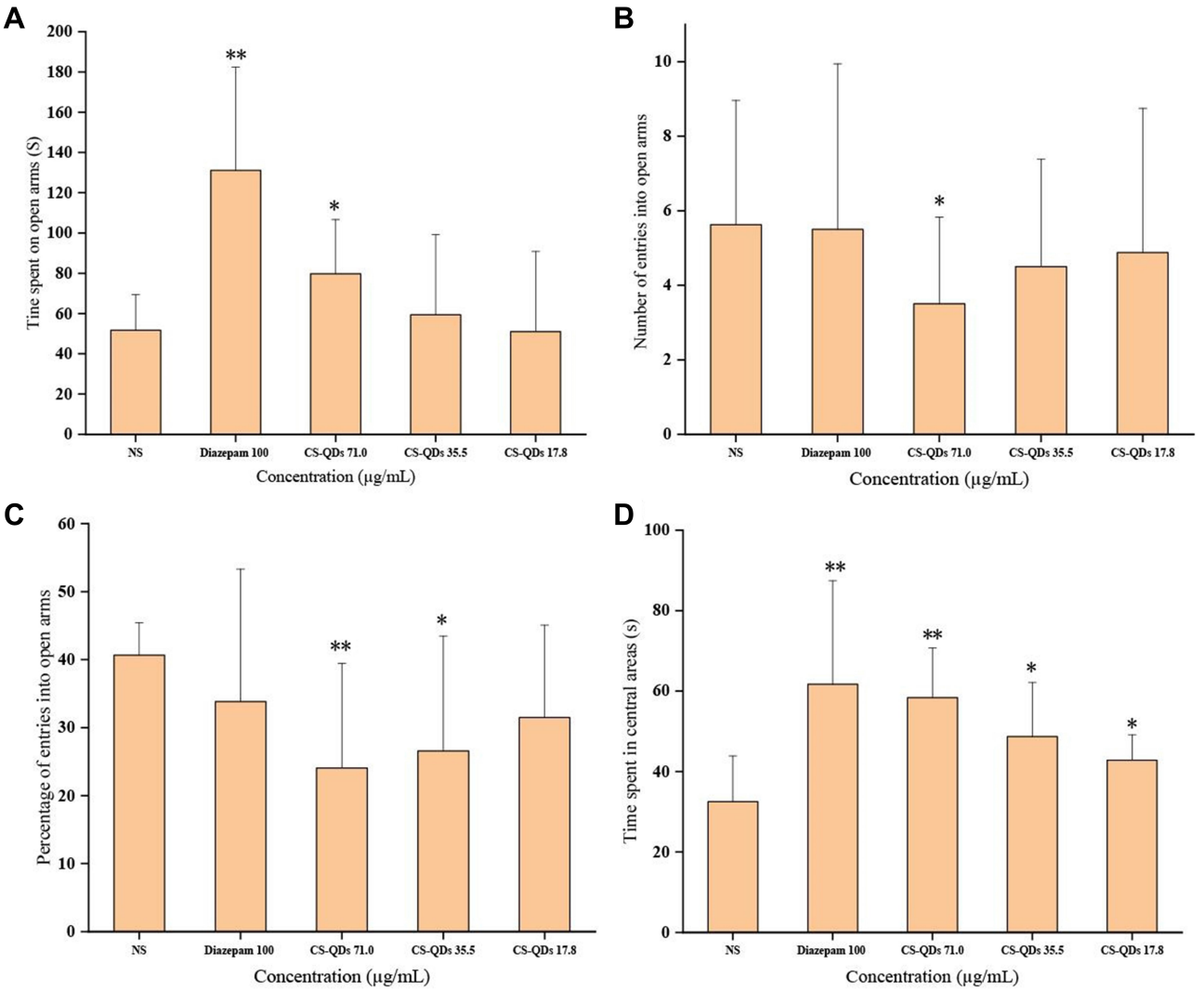

Figure 7 Effect of CS-CDs on the (**A**) time spent in the open arms of the elevated plus maze, (**B**) number of entries into open arms, (**C**) percentage of entries into open arms, and (**D**) time spent in the central area in the OFT. The results are presented as mean ± SD and significant difference compared with NS (*p<0.05; **p<0.01).

The results of the OFT are shown in Figure 7D. Mice in the groups that were administered 71 $\mu g \cdot mL^{-1}$ CS-CDs and 100 $\mu g \cdot mL^{-1}$ diazepam spent significantly more time in the central areas than those in the NS group ($p < 0.01$). Thus, there was a significant dose-dependent effect of CS-CDs on the time spent by mice in the central areas.

Effect of CS-CDs on Serum DA, CRH, ACTH, and CORT Concentrations

As shown in Figure 8, one-way ANOVA revealed no significant differences in the concentrations of CRH, ACTH, and CORT between groups. However, the concentrations of CRH, ACTH, and CORT in the CS-CDs (71 $\mu g \cdot mL^{-1}$) group were higher than those in the model group. Additionally, the concentrations of DA decreased significantly in the CS-CD group compared with those in the model groups.

Determination of Neurotransmitter Concentrations in Brain

Glu and GABA quantifications of mice brain were acquired via a UPLC-MS/MS; these results are shown in Figure 9A and B. After administration of the CS-CDs, the concentrations of Glu (Figure 9A) and GABA (Figure 9B) decreased in the brains of those groups compared with those in model groups, and the reduction of Glu reached significance.

Furthermore, the concentration of 5-HT and NE in mice brains were acquired using ELISA kits; these results

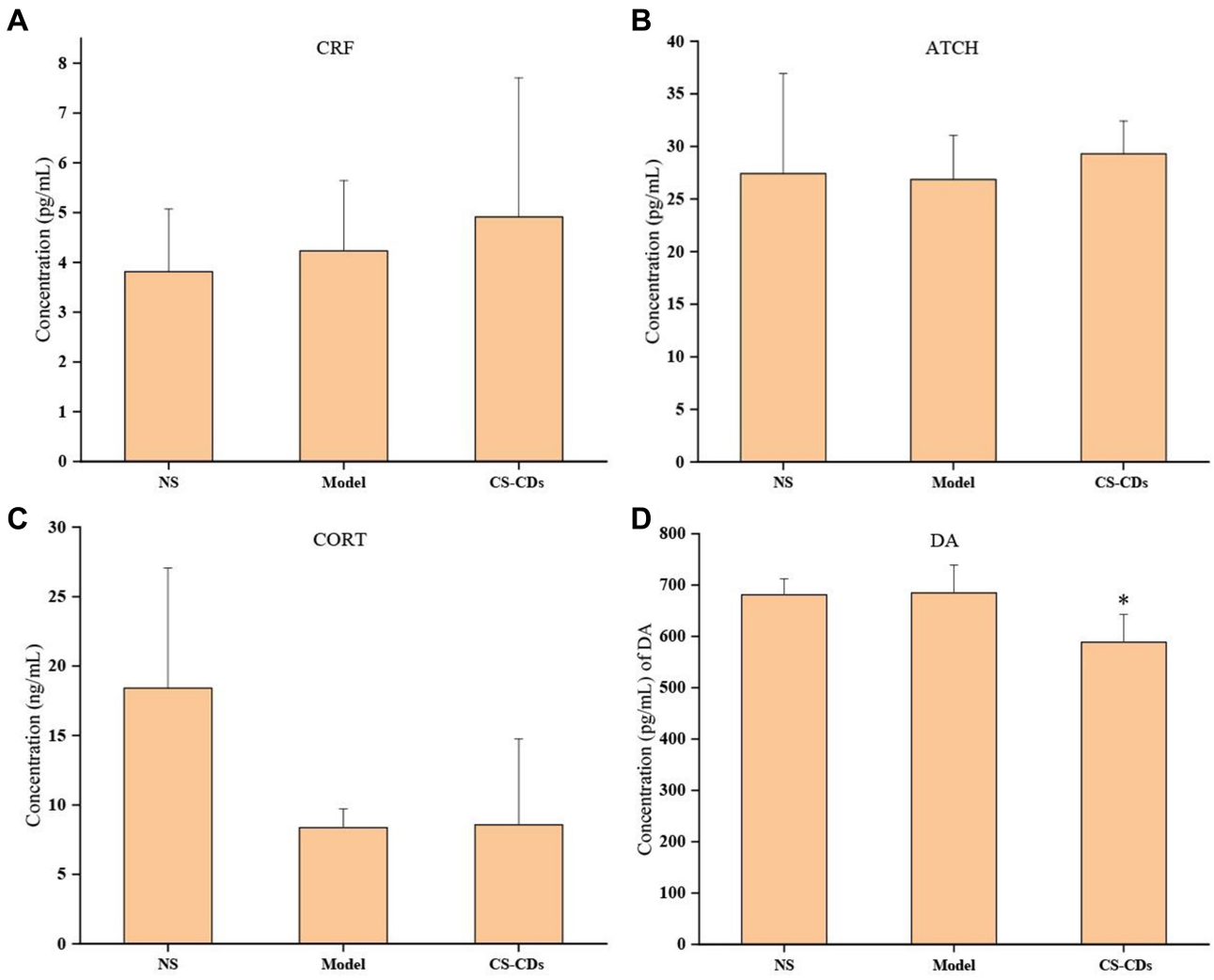

Figure 8 Effect of cigarettes smoke carbon dots (CS-CDs) on serum CRF (**A**), ACTH (**B**), CORT (**C**) and DA (**D**) after behavioural tests.

are shown in Figure 9C and D. The concentrations of NE (Figure 9D) in model groups considerably reduced compared with the NS groups and CS-CDs groups. The concentrations of 5-HT (Figure 9C) and NE followed the same change trend but were not significant.

Discussion

It is generally acknowledged that CS contains particulate material; however, previous studies have focused on investigating its chemical composition. To date, there are only a few particles reported among CDs from CS, and one reported that CS-CDs have broad-spectrum antimicrobial activities against drug-resistant bacteria.[17] The process of collecting CS between previous studies and our work is similar, which is common practice. However, after collection, in our study, extraction using ethyl acetate was performed, which removed fat-soluble components or fat-soluble CDs; therefore, the CDs prepared in our study were water-soluble, which is not the same as the CDs in previous work.

The identification methods of small molecular compounds developed from TCL to HPLC to UHPLC/ESI-Q-TOF-MS/MS.[42] In this study, although the absorption peak of CS-CDs could not be directly observed using the HPLC method, we demonstrated that the extracted and purified CS-CD solution did not contain nicotine or other small molecular compounds.

In general, nanoparticles with dimensions of 1–100 nm have a high surface area to volume ratio and possess unique physical and chemical properties. Nanoparticles have important biological applications, such as, in antibodies, membrane receptors, nucleic acids, and proteins. Therefore, nanoparticles have become a powerful tool in the field of medicine.[43] For example, oral efficacy can be improved by preparing a poorly soluble drug as

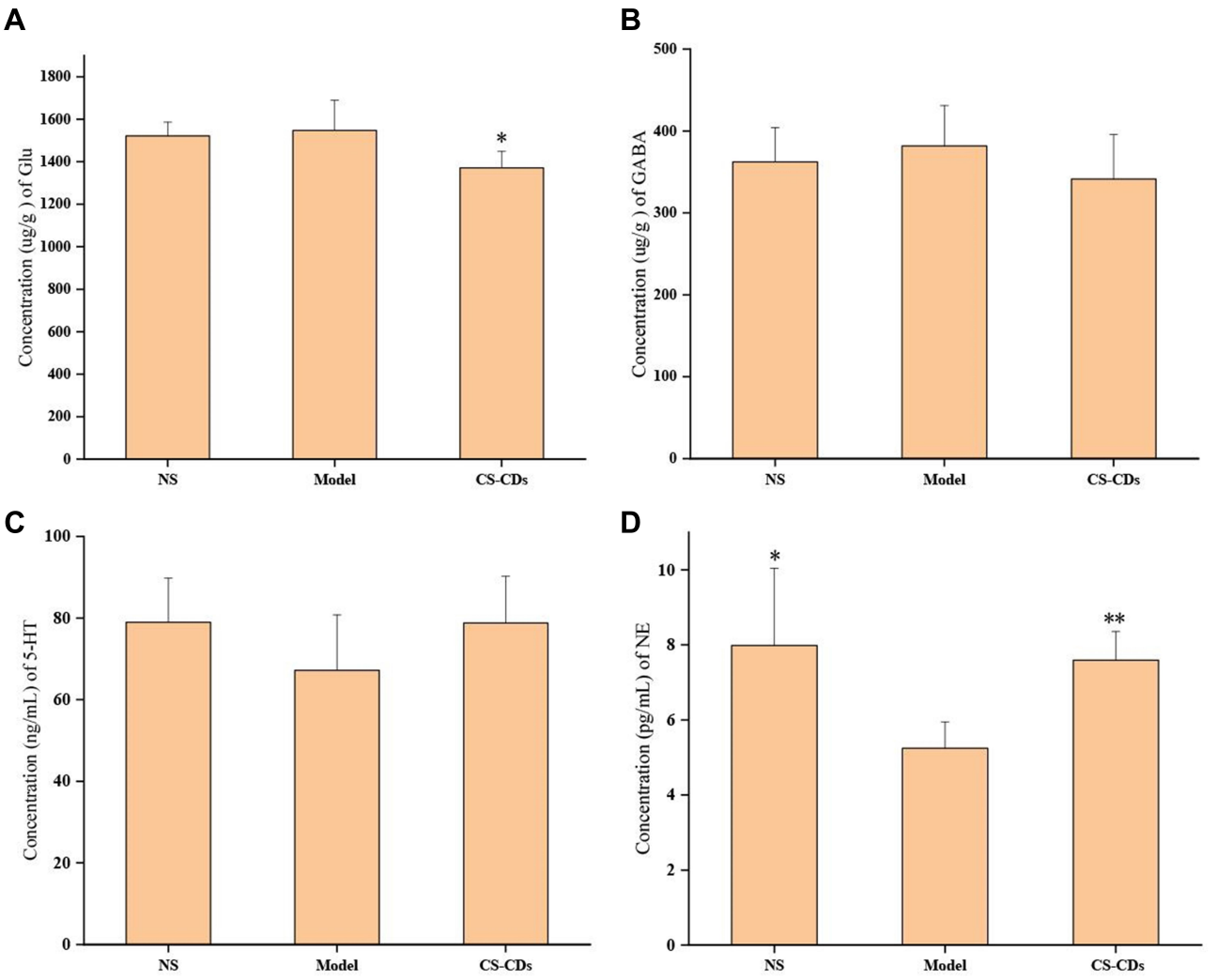

Figure 9 The concentration of Glu (**A**), GABA (**B**), 5-HT (**C**) and NE (**D**) in mice brains. The results are presented as mean ± SD and significant difference compared with model (*p<0.05; **p<0.01).

a nanoparticle.[43] In addition, drug targeting could be enhanced by preparing small molecular compounds in the form of nanoparticles.[44] CDs consist of nano-sized particles derived from carbon sources; CDs typically have sizes <10 nm, and have useful properties, such as biocompatibility, non-toxicity, and fluorescence. Thus, in recent years, due to their superior properties compared with other nanomaterials, CDs have been widely investigated for biomedical applications.[45]

Thus far, various carbon sources have been used to prepare CDs, such as by heating carbohydrates. Tan et al used plant soot as a carbon source for CD fabrication.[46] Hsu et al reported the preparation of CDs by heating coffee grounds.[47] CS-CDs are small carbon particles produced by the combustion of tobacco, which float in the air with smoke. The formation mechanism of CS-CDs is similar to that of coffee residue,[48] and it thought to involve the assembly of nicotine and other organic molecules due to hydrogen bonding. During cigarette burning, organic molecules undergo dehydration, polymerisation, and carbonisation, leading to a short single burst of nucleation; then, these nuclei grow by solute diffusion towards the particle surfaces.

In humans, smokers commonly report that they feel a reduction in stress after smoking. Quitting smoking can lead to anxiety, depression, or irritability,[6] which may be why people find it difficult to stop smoking. In particular, nicotine in cigarettes induces stimulation and pleasure, and reduces stress and anxiety.[5] Therefore, smokers use nicotine to modulate their level of arousal and for mood control in daily life. In addition, smoking may improve concentration, reaction times, and performance in certain

tasks.[5] To reduce the negative impact of smoking cessation, nicotine replacement therapy has been developed. Smoking cessation medications (including nicotine) do not increase the risk of serious cardiovascular events in the general population of smokers.[49] Additionally, nicotine affects the peripheral and central nervous systems, and increases heart rate and blood pressure while constricting cutaneous and coronary blood vessels.[50,51] Moreover, nicotine promotes DA secretion, making it addictive.[7] Thus, there are potential health safety concerns with nicotine replacement therapy.

When entering the body, nanoparticles may first interact with the immune system. They can be ingested by macrophages and concentrated in the lymph.[52,53] We selected RAW 264.7 cells, a widely used mouse macrophage cell line, for toxicity testing.[18] ICR mice were chosen because they are widely used in experiments, selected and bred by the Swiss mouse population for fertility, and used in central nervous system activity experiments.[54]

Our cytotoxicity tests showed that CS-CDs inhibited cell proliferation at high concentrations (71 $\mu g \cdot mL^{-1}$), which is consistent with the results in HepG2 cells (0.2–2 $mg \cdot mL^{-1}$),[55] but promoted cell proliferation at low concentrations in vitro. Notably, the cell viability was greater than 60% when the CS-CD concentration was less than 4.5 $\mu g \bullet mL^{-1}$, which may be desired (regeneration, neurogenesis, etc.) or undesired (tumours and cancers) cell proliferation. Because the type of cell proliferation is unknown, it is difficult to determine whether toxicity is high or low. Further study on cell proliferation is required. However, the results only indicated that the cytotoxicity of CS-CDs was low between 8.9 and 35.5 $\mu g \cdot mL^{-1}$. In addition, we found that the in vivo toxicity of the CS-CDs was low. Although no LD50 value was obtained in the acute toxicity test in vivo, there was no obvious toxicity at a 20× concentration of the purified solution.

EPMT and OFT are useful behaviour animal models to evaluate anxiolytics. In the EPMT, the time spent in the open arm is considered an indicator of anxiety; mice are less anxious if they spend more time in the open arms. Moreover, in the OFT, mice show less anxiety if they spend more time in the central areas. Diazepam is used as a standard drug for anxiety.[56] Smokers obtain a rapid feeling of emotional relief; therefore, assessment of the pharmacodynamics and mechanism of action should be performed in a short time after administration. In this study, we tested the anti-anxiety effect of CS-CDs at 10 min after administration to mimic the temporal effect of smoking. We found that the mice spent more time in the open arms and central areas when administrated CS-CDs or diazepam, demonstrating that CS-CDs are anxiolytic. Meanwhile, in the EPMT, the parameters that reflect the locomotor activity of mice decreased, thereby showing a certain sedative effect.

Central neurotransmitters mainly include monoamine neurotransmitters, amino acid neurotransmitters, peptides and other classes. Monoamine neurotransmitters include 5-HT, DA, NE, etc.; amino acid neurotransmitters include glycine, Glu, GABA, etc.; peptides include neuropeptides, P substances, vasopressin, cholecystokinin, CRF, etc. Neurons of monoamines, amino acids and peptide neurotransmitters are widely distributed in different brain regions and nuclei, and are involved in emotional regulation. 5- HT, NE, DA, GABA, and Glu in synaptic space changes are closely related to the occurrence and development of anxiety disorders. When a variety of causes lead to abnormal levels of neurotransmitters in the synaptic space, and transmitter transmission dysfunction, individuals show anxiety symptoms.[57,58] Acute stress triggers the release of CRF, ACTH, and CORT. CRF peptides play a critical role in the human stress response, and therefore, there has been increasing interest in investigating the potential pharmacological modulation of this system to reduce anxiety disorders.[59] To explore the mechanism of CS-CDs, we sacrificed the mice after EPMT and collected their serum and brain tissue to detect changes in neuroendocrine and neurotransmitter levels. The results showed that the concentrations of CRF, ACTH and CORT in the CS-CD groups were not significantly different from those in the model groups. However, CS-CDs promote the secretion of 5-HT and NE in the mouse brain; in particular, NE reached significance. In addition, the secretion of the excitatory amino acid Glu and the inhibitory amino acid GABA in the mouse brain decreased. It is noteworthy that the decrease in Glu secretion was faster than that of GABA. Additionally, CS-CDs significantly reduced the DA content in mouse serum. Therefore, overall, a trend of anti-anxiety was observed in the mice, which might be the mechanism for the anti-anxiety effect of CS-CDs. The decrease in Glu, DA and GABA secretion may be responsible for the sedative effect.

In summary, we isolated and purified a novel substance (CD) from CS, and described its anti-anxiety properties, chemical composition, and pharmacodynamics activity in

mice. In vitro and in vivo toxicity tests showed that CS-CDs had low toxicity. Anti-anxiety tests showed that CS-CDs reduced anxiety-like behaviour, similar to the effect of diazepam administration, and this effect was dose-dependent. Its mechanism causing anti-anxiety effects may be related to the decrease in Glu and DA and promotion of NE. Thus, our data suggest that the CS-CDs may be active components in CS that have anti-anxiety effects in smokers. In particular, CS-CDs could reduce dopamine production, making them less addictive, and may be a more valuable substitute for cigarette withdrawal.

Conclusion

Novel CDs were isolated and purified from CS (ie, CS-CDs). Acute toxicity testing in vitro and in vivo revealed that CS-CDs have low toxicity. The results of EPMT and OFT showed that CS-CDs had a significant anti-anxiety and a certain sedative effect on mouse behaviour. The mechanism for the anti-anxiety effect may be related to the decrease in Glu and DA and promotion of NE in the brain.

In conclusion, this study provides a new perspective towards a more comprehensive understanding of the components, properties, and functions of CS. The data we presented may offer a novel avenue for the development of smoking cessation substitutes and novel smoking cessation therapeutics.

Acknowledgments

We greatly appreciate the support of the Beijing key laboratory of Basic Research on Syndromes and Prescriptions and the Classical Prescription Basic Research Team of Beijing University of Chinese Medicine.

The authors thank Elsevier Professional Group Editing for providing language assistance and for proofreading the manuscript.

Disclosure

The authors declare that they have no conflicts of interest for this work.

References

1. World Health Organization (WHO), News release, Protocol to Eliminate Illicit Trade in Tobacco Products opened for signature. Available from: http://www.who.int/mediacentre/news/releases/2013/fctc20130110/en/. Accessed July 7, 2015.
2. Uchiyama S, Hayashida H, Izu R, Inaba Y, Nakagome H, Kunugita N. Determination of nicotine, tar, volatile organic compounds and carbonyls in mainstream cigarette smoke using a glass filter and a sorbent cartridge followed by the two-phase/one-pot elution method with carbon disulfide and methanol. *J Chromatogr A*. 2015;1426:48–55.
3. Baker RR. Pereira da Silva JR, Smith G. The effect of tobacco ingredients on smoke chemistry. Part I: flavourings and additives. *Food Chem Toxicol*. 2004;42(Suppl):S3–S37.
4. Thielen A, Klus H, Müller L. Tobacco smoke: unraveling a controversial subject. *Exp Toxicol Pathol*. 2008;60(2–3):141–156.
5. Benowitz NL. Pharmacology of nicotine: addiction, smoking-induced disease, and therapeutics. *Annu Rev Pharmacol Toxicol*. 2009;49:57–71.
6. Farris SG, Abrantes AM, Zvolensky MJ. Emotional distress and tobacco demand during the menstrual cycle in female smokers. *Cogn Behav Ther*. 2018;31:1–7.
7. Gaetano DC. Role of dopamine in the behavioural actions of nicotine related to addiction. *Eur J Pharmacol*. 2000;393(1–3):295–314.
8. Mishra V, Patil A, Thakur S, Kesharwani P. Carbon dots: emerging theranostic nanoarchitectures. *Drug Discov Today*. 2018;23(6):1219–1232.
9. Farshbaf M, Davaran S, Rahimi F, Annabi N, Salehi R, Akbarzadeh A. Carbon quantum dots: recent progresses on synthesis, surface modification and applications. *Artif Cells Nanomed Biotechnol*. 2018;46(7):1331–1348.
10. Li CL, Ou CM, Huang CC, et al. Carbon dots prepared from ginger exhibiting efficient inhibition of human hepatocellular carcinoma cells. *J Mater Chem B*. 2014;2(28):4564–4571.
11. Zhao Y, Zhang Y, Liu XM, et al. Novel carbon quantum dots from egg yolk oil and their haemostatic effects. *Sci Rep*. 2017;7(1):4452.
12. Zhang ML, Zhao Y, Cheng JJ, et al. Artif.Cells. Novel carbon dots derived from Schizonepetae Herba Carbonisata and investigation of their haemostatic efficacy. *Nanomed Biotechnol*. 2018;46(8):1562–1571.
13. Yan X, Zhao Y, Luo J, et al. Hemostatic bioactivity of novel Pollen Typhae Carbonisata-derived carbon quantum dots. *J Nanobiotechnology*. 2017;15(1):60.
14. Liu XM, Wang YZ, Yan X, et al. Novel Phellodendri Cortex (Huang Bo)-derived carbon dots and their hemostatic effect. *Nanomedicine*. 2018;13(4):391–405.
15. Wang YZ, Kong H, Liu XM, et al. Novel carbon dots derived from cirsii japonici herba carbonisata and their haemostatic effect. *J Biomed Nanotechnol*. 2018;14(9):1635–1644.
16. Sun ZW, Lu F, Cheng JJ, et al. Haemostatic bioactivity of novel Schizonepetae Spica Carbonisata-derived carbon dots via platelet counts elevation. *Artif Cells NanomedBiotechnol*. 2018;46(sup3):S308–S317.
17. Song YX, Lu F, Li H, et al. Degradable carbon dots from cigarette smoking with broad-spectrum antimicrobial activities against drug-resistant bacteria. *ACS Appl Bio Mater*. 2018;1(6):1871–1879.
18. Wang SN, Zhang Y, Kong H, et al. Antihyperuricemic and anti-gouty arthritis activities of Aurantii fructus immaturus carbonisata-derived carbon dots. *Nanomedicine*. 2019;14(22):2925–2939.
19. Lu F, Zhang Y, Cheng JJ, et al. Maltase and sucrase inhibitory activities and hypoglycemic effects of carbon dots derived from charred Fructus crataegi. *Mater Res Express*. 2019;6(12):125005.
20. Wang XK, Zhang Y, Zhang ML, et al. Novel carbon dots derived from puerariae lobatae radix and their anti-gout effects. *Molecules*. 2019;24:E4152.
21. Zhang ML, Cheng JJ, Sun ZW, et al. Protective effects of carbon dots derived from phellodendri chinensis cortex carbonisata against deinagkistrodon acutus venom-induced acute kidney injury. *Nanoscale Res Lett*. 2019;14(1):377.
22. Xue X, Yang JY, He Y, et al. Aggregated single-walled carbon nanotubes attenuate the behavioural and neurochemical effects of methamphetamine in mice. *Nat Nanotechnol*. 2016;11(7):613–620.
23. Fang J, Liu Y, Chen Y, Ouyang D, Yang G, Yu T. Graphene quantum dots-gated hollow mesoporous carbon nanoplatform for targeting drug delivery and synergistic chemo-photothermal therapy. *Int J Nanomed*. 2018;13:5991–6007.
24. Zhang F, Xiao CT, Li YF, et al. Gram-scale synthesis of blue-emitting CH(3)NH(3)PbBr(3) Quantum Dots Through Phase Transfer Strategy. *Front Chem*. 2018;6:444.

25. Dobhal G, Ayupova D, Laufersky G, Ayed Z, Nann T, Goreham RV. Cadmium-Free Quantum Dots as Fluorescent Labels for Exosomes. *Sensors*. 2018;18(10):pii: E3308.
26. Bai Y, Zhang B, Chen L, et al. Synthesis of polydopamine carbon dots for photothermal therapy. *Nanoscale Res Lett*. 2018;13(1):287.
27. Keinänen M, Oldham NJ, Baldwin IT. Rapid HPLC screening of jasmonate-induced increases in tobacco alkaloids, phenolics, and diterpene glycosides in Nicotiana attenuata. *J Agric Food Chem*. 2001;49(8):3553–3558.
28. Hu SL, Niu KY, Sun J, Yang J, Zhao NQ, Du XW. One-step synthesis of fluorescent carbon nanoparticles by laser irradiation. *J Mater Chem*. 2009;19:484–488.
29. Li C, Zhang P, Hao Y, He D, Shen Y, Lu R. Expression and significance of quantum dots in RAW 264.7 macrophages. *Oncol Lett*. 2018;16(5):5997–6002.
30. Misik J, Pavlikova R, Cabal J, Kuca K. Acute toxicity of some nerve agents and pesticides in rats. *Drug Chem Toxicol*. 2015;38(1):32–36.
31. Liu J, Lv YW. Anti-Anxiety Effect of (-)-Syringaresnol-4-O-β-d-apiofuranosyl-(1→2)-β-d-glucopyranoside from Albizzia julibrissin Durazz (Leguminosae). *Molecules*. 2017;22:8.
32. Santos P, Herrmann AP, Benvenutti R, et al. Anxiolytic properties of N-acetylcysteine in mice. *Behav Brain Res*. 2017;317:461–469.
33. Bourlinos AB, Georgakilas V, Zboril R, et al. Pyrolytic formation and photoluminescence properties of a new layered carbonaceous material with graphite oxide-mimicking characteristics. *Carbon*. 2009;47 (2):519–526.
34. Sachdev A, Gopinath P. Green synthesis of multifunctional carbon dots from coriander leaves and their potential application as antioxidants, sensors and bioimaging agents. *Analyst*. 2015;140(12):42 60–4269.
35. Fang YX, Guo SJ, Li D, et al. Easy synthesis and imaging applications of cross-linked green fluorescent hollow carbon nanoparticles. *ACS Nano*. 2012;6(1):400–409.
36. Zhu C, Yang SW, Wang G, et al. A new mild, clean and high-efficient method for preparation of graphene quantum dots without by-products. *J Mater Chem B*. 2015;3(34):6871–6876.
37. Chiu SH, Gedda G, Girma WM. Rapid fabrication of carbon quantum dots as multifunctional nanovehicles for dual-modal targeted imaging and chemotherapy. *Acta Biomater*. 2016;46:151–164.
38. Moniuszko G, Skoneczny M, Zientara-Rytter K, et al. LSU-like protein couples sulphur-deficiency response with ethylene signalling pathway. J. *Exp Bot*. 2013;64(16):5173–5182.
39. Sabet MS, Zamani K, Lohrasebi T, Malboobi MA, Valizadeh M. Functional assessment of an overexpressed arabidopsis purple acid phosphatase gene (AtPAP26) in Tobacco Plants. *Iran J Biotechnol*. 2018;16(1):e2024.
40. Zhao SY, Liu J, Li CX, et al. Tunable Ternary (N, P, B)-Doped porous nanocarbons and their catalytic properties for oxygen reduction reaction. *ACS Appl Mater Inter*. 2014;6(24):22297–22304.
41. Sun D, Ban R, Zhang PH, Wu GH, Zhang JR, Zhu JJ. Hair fiber as a precursor for synthesizing of sulfur- and nitrogen-co-doped carbon dots with tunable luminescence properties. *Carbon*. 2013;64 (Complete):424–434.
42. Ahmad N, Ahmad R, Al-layly A, et al. Ultra-high-performance liquid chromatography-based identification and quantification of thymoquinone in Nigella sativa extract from different geographical regions. *Pharmacogn Mag*. 2018;14(57):471–480.
43. Bamburowicz-Klimkowska M, Poplawska M, Grudzinski IP. Nanocomposites as biomolecules delivery agents in nanomedicine. *J.Nanobiotechnology*. 2019;17(1):48.
44. Ahmad N. Rasagiline-encapsulated chitosan-coated PLGA nanoparticles targeted to the brain in the treatment of parkinson's disease. *J Liq Chromatogr R T*. 2017;40(13):677–690.
45. Jaleel JA, Pramod K. Artful and multifaceted applications of carbon dot in biomedicine. *J Control Release*. 2018;269:302–321.
46. Tan MQ, Zhang LX, Tang R, et al. Enhanced photoluminescence and characterization of multicolor carbon dots using plant soot as a carbon source. *Talanta*. 2013;115(Complete):950–956.
47. Hsu PC, Shih ZY, Lee CH, Chang HT. Synthesis and analytical applications of photoluminescent carbon nanodots. *Green Chem*. 2012;14(4):917–920.
48. Ray SC. Fluorescent carbon nanoparticles: synthesis, characterization, and bioimaging application. *J Phys Chem C*. 2009;113 (43):18546–18551.
49. Benowitz NL, Pipe A, West R, et al. Cardiovascular safety of varenicline, bupropion, and nicotine patch in smokers: a randomized clinical trial. *JAMA Intern Med*. 2018;178(5):622–631.
50. Schroeder MJ, Hoffman AC. Electronic cigarettes and nicotine clinical pharmacology. *Tob Control*. 2014;Suppl 2:ii30.
51. Smith TT, Rupprecht LE, Sved AF, Donny EC. Characterizing the relationship between increases in the cost of nicotine and decreases in nicotine content in adult male rats: implications for tobacco regulation. *Psychopharmacology*. 2016;233(23–24):3953–3964.
52. Riviere JE. Pharmacokinetics of nanomaterials: an overview of carbon nanotubes, fullerenes and quantum dots. *Wiley Interdiscip Rev Nanomed Nanobiotechnol*. 2009;1(1):26–34.
53. Zhao Y, Zhang Y, Qin G, et al. In vivo biodistribution and behavior of CdTe/ZnS quantum dots. *Int J Nanomedicine*. 2017;12:1927–1939.
54. Silva MI, de Aquino Neto MR, Teixeira Neto PF, Moura BA. do Amaral JF, de Sousa DP, Vasconcelos SM, de Sousa FC. Central nervous system activity of acute administration of isopulegol in mice. *Pharmacol Biochem Behav*. 2007;88(2):141–147.
55. Na X, Zhang L, Wang H, Tan M. Adverse effect assessment of fluorescent carbon dots in cigarette smoke. *Nanoimpact*. 2020; 19:100241.
56. Nishioka Y, Oyagi A, Tsuruma K, Shimazawa M, Ishibashi T, Hara H. The antianxiety-like effect of astaxanthin extracted from Paracoccus carotinifaciens. *Biofactors*. 2011;37(1):25–30.
57. Nikolaus S, Antke C, Beu M. striatal dopamine and midbrain serotonin as the key players in compulsive and anxiety disorders–results from in vivo imaging studies. *Rev Neurosci*. 2010;21(2):119–139.
58. Maron E, Nutt D. Biological markers of generalized anxiety disorder. *Dialogues Clin Neurosci*. 2017;19(2):147–158.
59. Kent JM, Mathew SJ, Gorman JM. Molecular targets in the treatment of anxiety. *Biol Psychiatry*. 2002;52(10):1008–1030.